2007

Raman Spectroscopic Study Of Single Red Blood Cells Infected By The Malaria Parasite Plasmodium Falciparum

William Carter
University of Central Florida

RAMAN SPECTROSCOPIC STUDY OF SINGLE RED BLOOD CELLS INFECTED BY THE MALARIA PARASITE PLASMODIUM FALCIPARUM

by

WILLIAM D CARTER III
B.S. University of Central Florida, 1996

A thesis submitted in partial fulfillment of the requirements
for the degree of Master in Science
in the Department of Physics
in the College of Sciences
at the University of Central Florida
Orlando, Florida

Summer Term
2007

ABSTRACT

Raman micro-spectroscopy provides a non-destructive probe with potential applications as a diagnostic tool for cellular disorders. This study presents micro-Raman spectra of live erythrocytes infected with a malaria parasite and investigates the potential of this probe to monitor molecular changes which occur during differentiation of the parasite inside the cell. At an excitation wavelength of 633 nm the spectral bands are dominated by hemoglobin vibrations yielding information the on structure and spin state of the heme moiety. It also demonstrates the novel use of silica capillaries as a viable method for studying the erythrocytes in an environment that is much closer to their native state, thus opening the possibility of maintaining the cell *in vivo* for long periods to study the dynamics of the parasite's growth.

ACKNOWLEDGMENTS

I would like to thank my advisor, Dr. Alfons Schulte for providing this wonderful opportunity to work with him. I am grateful to him for spending so much of his valuable time with me throughout this project and guiding me along the way.

I would like to thank Dr. Debopam Chakrabarti and his research group for their assistance by providing their Molecular Biology and Parasitology experience to a Physics major. Also, I would like to thank Lawrence Ayong for his assistance by being available to provide samples on short notice.

I also thank Dr. Lee Chow for being a member of my thesis committee.

I would also like to thank Dr. Eduardo Mucciolo for his assistance with my return to the University after so many years. He went above and beyond in helping with paperwork and petitions while I was still away overseas. Without his assistance this thesis would not have been possible.

Finally, I thank my parents for their encouragement always believing in me.

TABLE OF CONTENTS

LIST OF FIGURES

LIST OF TABLES

CHAPTER ONE: INTRODUCTION

Malaria

Summary

Malaria is a leading cause of sickness and death in areas endemic for the parasites *Plasmodium falciparum*, *Plasmodium vivax*, *Plasmodium malariae*, and *Plasmodium ovale*. Up to 1 million people die each year from malaria, most of them African children [1]. Between 400 million and 900 million cases of acute malaria occur annually in African children alone [2]. According to the U.S. Center for Disease Control and Prevention, more than 1,400 new cases are reported annually in the United States in travelers returning from malaria-endemic areas [1].

The human malaria parasite has a complex life cycle that requires both a human host and an insect host. In *Anopheles* mosquitoes, Plasmodium reproduces sexually (by merging of the parasite's sex cells). In humans the parasite reproduces asexually (by cell division), first in liver cells and then in red blood cells. When an infected female *Anopheles* mosquito bites a human, she injects saliva containing the parasite in its sporozoite form into the person's bloodstream. The sporozoite promptly invades a liver cell. There, during the next 7-14 days (depending on the species of the parasite), each sporozoite develops into a schizont, a structure that contains thousands of tiny rounded merozoites (another stage of the parasite). When the schizont matures, it ruptures and releases the merozoites into the bloodstream. Merozoites released from the liver invade red blood cells where they consume hemoglobin, the oxygen-carrying part of the blood. Within the red blood cell, most merozoites go through yet another round of asexual reproduction, again forming schizonts filled with more merozoites. When these schizonts mature, the cell ruptures and the merozoites burst out. The newly released merozoites invade

other red blood cells, and the infection continues its cycle until it is brought under control either by medicine or the body's immune defenses. The *Plasmodium* parasite can complete its life cycle through the mosquito because some of the merozoites that penetrate red blood cells do not develop asexually into schizonts. Rather, they change into male and female sexual forms known as gametocytes. These circulate in the person's bloodstream, awaiting the arrival of another blood-seeking female *Anopheles* [2].

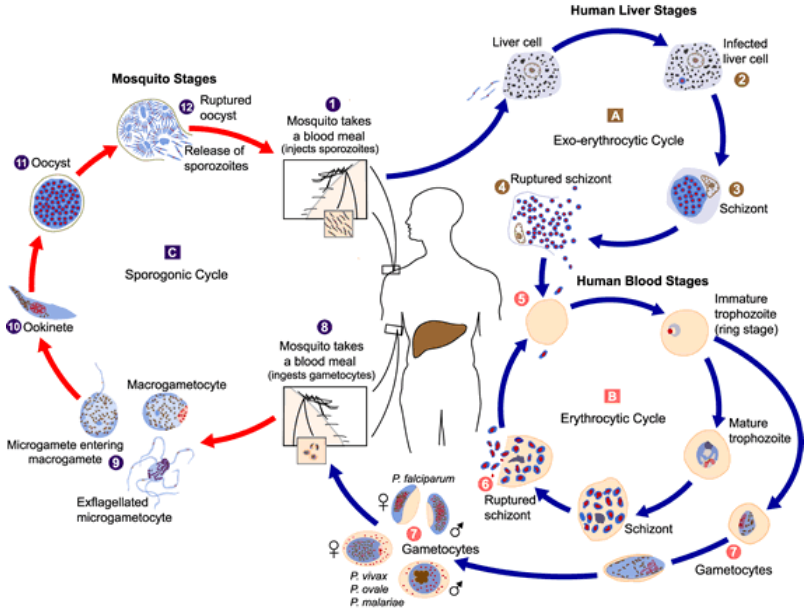

Figure 1: Life cycle of P. falciparum [3]

When the mosquito bites an infected person, she sucks up gametocytes along with blood. Once in the mosquito's stomach, the gametocytes develop into sperm-like male gametes or large, egg-like female gametes. Fertilization produces an oocyst filled with infectious sporozoites. When the oocyst matures, it ruptures and the thread-like sporozoites migrate, by the thousands, to the mosquito's salivary (saliva-producing) glands. And the cycle starts over again when she bites her next victim [2].

Current Techniques for Diagnosis of Malaria

A doctor or other health care worker should suspect malaria whenever a person who has been in the tropics recently or received a blood transfusion develops a fever and other signs that resemble the flu. A doctor will examine blood smears under a microscope. If parasites are present, the diagnosis is confirmed. A "thick" smear makes it possible for the health care worker to examine a large amount of blood. Then, the species of parasite can be identified by looking at a corresponding "thin" smear. This is important for deciding on the best treatment [4]. Mixed infections are possible. For example, a person can be infected with *P. vivax* as well as the more dangerous *P. falciparum* [1]. In the unusual event that parasites cannot be seen immediately in a blood smear, but the patient's condition and prior activities strongly suggest malaria, the doctor may decide to start treatment before being sure the patient has malaria. Any detection of Malaria is considered a medical emergency and delays in starting treatment are the leading cause of death [1].

Figure 2: Field technician using light microscopy for malaria diagnosis [5]

Using light microscopy with a 100x oil-immersion objective of a well stained thick blood smear remains the standard technique for detecting malaria parasites. It can detect densities as

low as 5–10 parasites per micro liter when used by skilled technicians or 100 parasites per micro liter under field conditions by a typical technician. However, the process is time consuming and depends on good reagents, equipment and, most importantly, well-trained and skilled technicians. These conditions are often not met, particularly at the more peripheral levels of the health-care system [6].

A Spectroscopic Solution

Understanding the life cycle of the parasite is essential to studying it. When the parasite develops within a human red blood cell it causes hemoglobin degradation and heme crystallization into a non-toxic compound called hemozoin. Raman micro-spectroscopy achieves chemically selective imaging of the living cell using the vibrational signatures of molecules. The vibrational bands (shape, position, intensity) provide information on protein configuration, heme structure, and molecular structural changes. Looking for these characteristics of the hemozoin vibrational structure will lead to a Raman method for diagnosis of malaria.

In addition to simply being a diagnostic tool, another important feature of this work is the novel use of the capillaries to study the cells. The ability to study both infected and uninfected cells in an environment more closely resembling their native environment would be very beneficial, not only for the diagnosis of malaria but for the study of any biological sample. It will allow for future studies to observe the cells alive in a homeostatic environment and, by keeping the cell/parasite alive, allow for the same cell to be studied over the life cycle of either the cell or its infecting parasite. This may lead to a clearer understanding of the hemoglobin degradation process and provide data that will be useful in the development of anti-malarial therapies.

Relevant Raman Research Topics

Raman in Biochemical Analysis

Recent years have seen a growing use of Raman in the study of biological systems. With advances in laser sources, Rayleigh rejection filters, and detector technology, the weak Raman signal is easier to detect and analyze. Raman spectroscopy is currently being used for such applications as tissue diagnostics, blood analyte detection, and cellular examination, among others. The greatest benefit of using this technique is due to its sensitivity to very subtle molecular changes as well as its capability for non-invasive sensing. In addition, Raman offers generally narrow bandwidths, minimal sample preparation, and is easily integrated with microscopes to provide very small spatial resolution [7].

There are other advantages of Raman spectroscopy over other single cell techniques. There exists the possibility of analyzing biological system *in vivo* because aqueous solutions are weak Raman scatterers. Markers/dyes are not necessary and allow for faster sample preparation. It removes some of the human error by providing an automated method of analysis. The lab technician no longer needs to rely on visual inspection of cells. The also allows for dynamics to be monitored without the need of the technician to continuously watch the cell under investigation.

Micro-Raman Spectra of Hemoglobin

The use of Raman spectroscopy to study red blood cells is not new. Wood and McNaughton showed in 2002 that a clear difference existed in the spectra taken from oxygenated and deoxygenated cells. The study was conducted using different wavelength of excitation radiation (488nm, 514nm, 568nm, and 632nm). It was shown that the excitation wavelength had a definite

impact on the resulting spectra. They hypothesized that the use of 632.8 nm radiation would be the best to use as a non-destructive probe in the investigation of cellular disorders. This wavelength is well below the fluorescence range, it seemed to show the most detailed structures, and is of low enough energy to avoid damage to the cell under investigation [8]. In addition, the simplicity and widespread availability of He-Ne lasers system make it a good choice for a diagnostic system that must be robust enough for field work.

Raman Spectroscopy in Malaria Research

It has been shown that during the intra-cellular phase of the malaria parasite's life cycle that the parasite degrades up to 75% of the cells hemoglobin [9]. While hemoglobin proteolysis yields requisite amino acids, it also releases toxic free-heme which can kill the parasite by disrupting cell membranes. To protect itself against the toxic effects of free-heme, the malaria parasites have evolved a detoxification method which involves the formation of a crystallized hemozoin [2]. This hemozoin has been shown to be identical in structure to the synthetic material β-hematin. This aggregate heme product has a distinct Raman spectrum and can be detected [11]. This spectrum is very similar to that of hemoglobin due to the strong Raman activity of the heme moiety. Using this as a naturally occurring marker, a method of detecting malaria through spectroscopy is possible.

Intent of this Research

Raman Spectroscopy as a Diagnostic Tool

It is the goal of this paper to show the potential use of Raman Spectroscopy as a non-destructive probe in the diagnosis of Malaria. It will first concentrate on the set up of the system by comparison with previous work from the literature. The measurement of spectra in live red

blood cells will be taken using 632.8 nm radiation. This will be followed by taken spectra from red blood cells infected with the malaria parasite using the same set up. An analysis of the spectra will be completed, primarily looking for shift in peaks associated with the heme separation from the hemoglobin and the formation of hemozoin.

Benefits of Capillary Sample Preparation

The technique will be expanded to include data collected using glass capillaries. An analysis of the capillary data will be conducted to show the potential usefulness of the technique. The use of capillaries to maintain the cells and parasite in a live state for continued study as the parasite develops will be discussed. The possibilities that this capillary technique opens up for use in the field as a tool for the healthcare worker will also be described.

Expectations

It is expected that the samples taken on traditional glass slide will agree with previously published data thus verifying the accuracy and capability of the experimental set up. The ability to target specific volumes within in the cell should be successful and clearly show the presence of the malaria parasite by the detection of the hemoglobin spectra. Finally, the use of the capillaries should show that near identical spectra can be obtained and that the preparation of the sample will be much simpler than the slides and allow for the repeated study of the same cell is possible.

CHAPTER TWO: BACKGROUND

The Raman Effect

Light incident on some material will be scattered. This scattering can be inelastic (Rayleigh) or elastic (Raman). The inelastically scattered light undergoes no transfer of energy and therefore has the same wavelength as the incident light. The elastically scattered light does exchange energy with the atoms of the scattering material and thus the wavelength of this scattered light is shifted by some certain amount. This shift is known as the Raman shift after its discoverer C. V. Raman and is characteristic of the vibrational modes in the material. It is an excellent tool for probing the molecular structure of the material [10].

The Raman Effect can be explained through a classical treatment of the electromagnetic wave of the incident beam and will be described first. A brief quantum description will follow.

Classical Description of Raman Scattering

By considering the bound atoms in a molecule as point nuclei and the bonds between them as springs it can be shown that there are 3N-5 possible vibrational modes (3N-6 for linear molecules) where N is the number of atoms. The assumption is that the molecule's diameter is much less that the wavelength of the incident monochromatic light (to assure that it "sees" a homogenous field.) The field then induces a dipole moment in the molecule and as such a polarization given by Eq. 2-1.

$$P(t) = \alpha E(t) \tag{2-1}$$

The incident field can be written as a simple oscillating function with peak amplitude E_0 and a frequency ν_{inc} (Eq. 2-2). The response of the atoms will be to displace from their equilibrium positions.

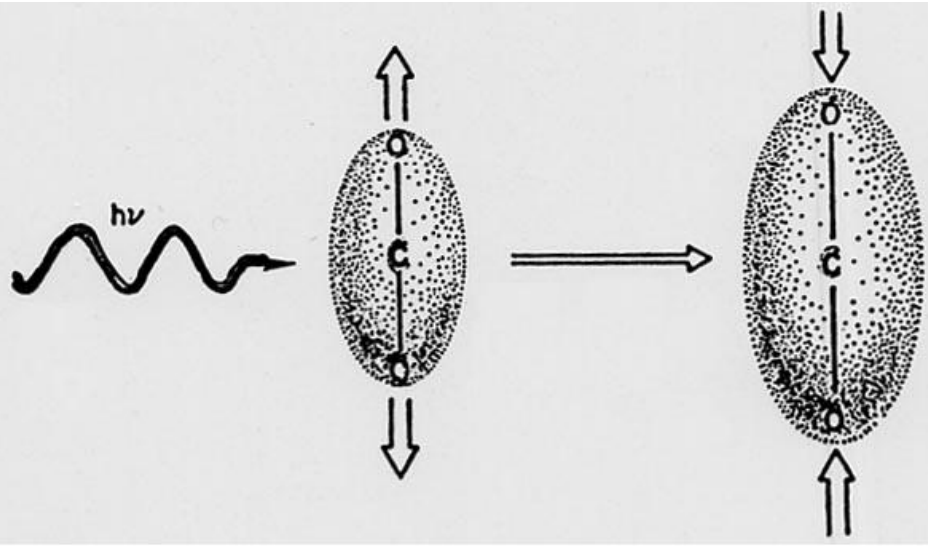

Figure 3: Light induced polarization

$$E(t) = E_0 \cos(2\pi\nu_{inc} t) \tag{2-2}$$

The atoms' displacement can be described by a normal coordinate q_j (with the subscript indicating the vibrational mode.) The mode is assumed to oscillate although not necessarily with the same frequency (Eq. 2-3).

$$q_j(t) = q_j^{(0)} \cos(2\pi\nu_j t) \tag{2-3}$$

The polarizability of the electrons in the molecule can be written out as a Taylor series (Eq. 2-4). The induced dipole moment due to the vibrational modes is then given by:

$$\alpha = \alpha_0 + \left(\frac{\partial\alpha}{\partial q_j}\right) q_j + \ldots \tag{2-4}$$

Simply substituting these equations into 2-1 gives:

$$P(t) = \left[\alpha_0 + \left(\frac{\partial\alpha}{\partial q_j}\right) q_j\right] E_0 \cos(2\pi\nu_{inc} t)$$

$$P(t) = \alpha_0 E_0 \cos(2\pi\nu_{inc} t) + \left(\frac{\partial \alpha}{\partial q_j}\right) q_j^{(0)} \cos(2\pi\nu_j t) E_0 \cos(2\pi\nu_{inc} t)$$

By using the trigonometric identity for the product of cosines:

$$P(t) = \alpha_0 E_0 \cos(2\pi\nu_{inc} t) + \frac{E_0 q_j^{(0)}}{2}\left(\frac{\partial \alpha}{\partial q_j}\right)\left[\cos(2\pi(\nu_{inc} + \nu_j)t) + \cos(2\pi(\nu_{inc} - \nu_j)t)\right] \quad (2\text{-}5)$$

Eq. 2-5 shows that the response of the molecule to the incident radiation has a term that responds with the same frequency as that radiation. This term corresponds to Rayleigh scattering. The next, much weaker term, is a frequency response that reacts with two components, one as the sum of the two frequencies and one as the difference. These correspond to the anti-Stokes Raman scattering and the Stokes Raman scattering respectively [10].

Although this derivation is classical and therefore incomplete, it does highlight most of the important features. First, both the Rayleigh and Raman scattering are linear with input intensity. Second, only vibrations that affect the polarizability exhibit Raman scattering (the Raman scattering selection rule.) Finally, it shows that the Raman shift can be either positive or negative. All of these same features are derived from the quantum description as well many others [11].

Quantum Description of Raman Scattering

Although the classical description of light scattering does reveal most of the important characteristics that are necessary to make use of the phenomena for spectroscopy, it is limited because it fails to take into account the quantum nature of molecular systems. It is worth briefly verifying the classical calculations with quantum methods. Using basic second order time-dependent perturbation theory and applying it to virtual vibrational states it gives a good first

order quantum description of both Rayleigh and Raman scattering [13]. A complete description would treat the molecule as a quantum particle and would have to include relativistic effects as well as treating the incident radiation quantum mechanically. Both of these are not necessary to uncover all of the phenomena needed to use the Raman Effect as a spectroscopic tool and are beyond the scope covered here.

The incident radiation is treated as a perturbation to the eigenstates of the molecule. This perturbation creates virtual vibrational states (as opposed to electronic states.) The incident photon excites the ground state, for example, to this virtual state as shown in Figure 3. This state can decay back down to the original state with no net change in energy (Rayleigh scattering.) The state can also decay to a state just above or below the original resulting in an emitted photon that has either slightly more or less energy. This energy difference in the emitted photon is then due to the spread in energy level within the vibrational level and corresponds to the Raman shift.

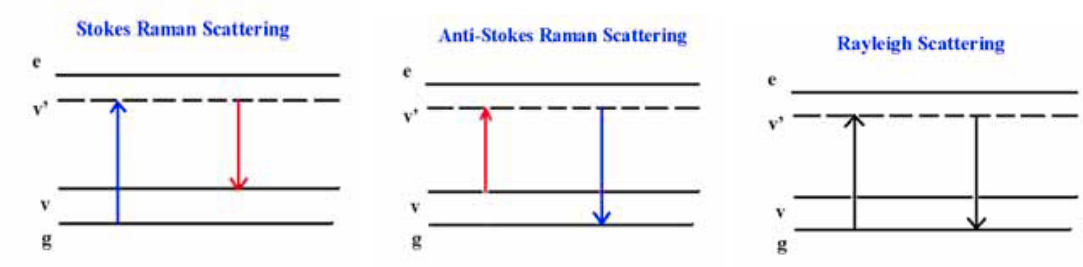

Figure 4: Stokes, Anti-Stokes, and Rayleigh scattering [12]

A more rigorous derivation of the concepts can be seen if the ground state is written as $|g\rangle$ and the virtual state as $|r\rangle$. The Hamiltonian for the system is the sum of the the electric dipole, the magnetic dipole, electric quadrupole, and higher order terms (equation 2-6.)

$$\hat{H} = \hat{H}_p + \hat{H}_m + \hat{H}_\theta + \ldots \qquad (2\text{-}6)$$

Only the electric dipole will be considered here. The higher order effects are sufficiently small when the field is taken as constant over the length of the normal coordinate. This is a valid assumption when the incident radiation is in the visible region or longer and the bond lengths are on the order of angstroms ($\lambda_{inc} \approx 6000\,nm >> 1-5\text{Å}$).

Using second order time-dependent perturbation theory, the polarizability of the molecule in this state is given by Eq 2-7.

$$\alpha^g = \frac{2}{\hbar}\sum_r \frac{\nu_{rg}\left|\langle r|\hat{M}|g\rangle\right|^2}{\nu_{rg}^2 - \nu_{inc}^2} \tag{2-7}$$

The operator *M* determines the probability of a specific transition occurring and comes from the transition dipole moment. From this an analogous equation to 2-4 can be written for the quantum description.

$$\alpha_{gn}(t) = \langle n|\alpha|g\rangle + \sum_k \left(\alpha_{gn}\right)_k \langle n|q_k|g\rangle \tag{2-8}$$

Due to the orthogonality of the states the first term is zero unless the two states are the same. This corresponds to Rayleigh scattering. The second term is then non-zero only when $n = m \pm 1$, for any given vibrational mode *k*. The +1 term corresponds to Stokes scattering. The -1 term corresponds to Anti-Stokes scattering. These terms can be evaluated to determine actual probabilities for specific transitions to occur.

This brings to light one of the shortcomings of the classical derivation; namely that the transition from the ground state can not produce Anti-Stokes scattering and therefore, due to the Boltzmann distribution of states, will occur much less frequently than the Stoke transition. Another feature that the classical derivation fails to recognize is the quantized nature of rotation and vibrations.

Micro-Raman Spectroscopy

Basics

Combining a Raman set up with a microscope allows for the spectroscopic sampling of very small volumes. Because the volumes are small very little Raman signal is necessary for detection and therefore the power of the input source can be kept low. This is an ideal tool for biological systems where the targets are small (on the cellular level) and optical damage can occur at very low laser power levels. Keeping the sample undamaged is a requirement for repeated experiments but also to study dynamic variables in a biological system.

The basic set up is shown in Figure 5. The laser and detector are on the same side of the sample in what is called 180º geometry [10]. A beam splitter is used to insert the laser into the collection axis. The backscattered light reflects from the sample and then passes through the beam splitter to the detector. The spatial resolution of the system is then limited by the laser and objective lens.

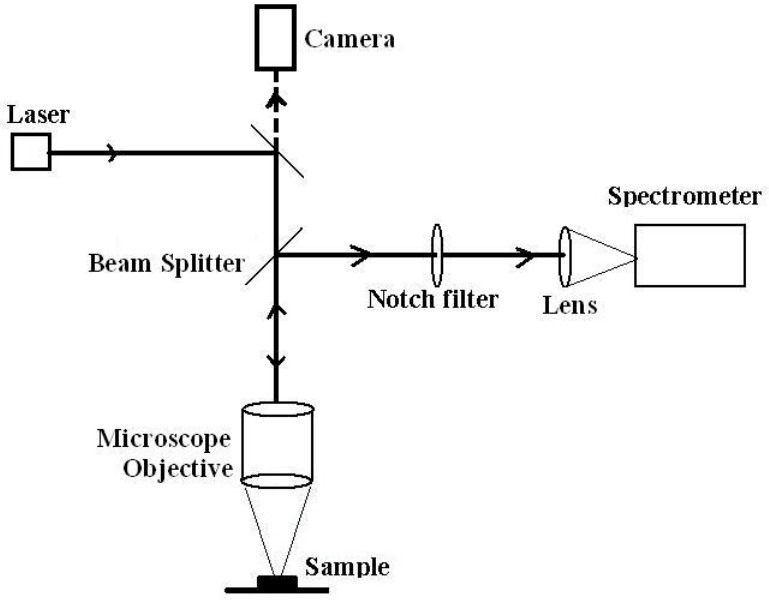

Figure 5: Micro Raman setup schematic [13]

Using a Raman microscope the sample can simply be placed on a three dimensionally translational stage and the portion of the samples that is of interest is selected optically through the viewing system of the microscope. With micro-Raman the vibrational spectra can be measured form micron-sized particles which makes it well suited as an analytical tool in chemistry and biotechnology. Raman micro-spectroscopy has proven to be an informative and nondestructive technique.

Hemoglobin Degradation by the Malaria Parasite

Hemoglobin Degradation

There are several reasons suspected for the parasite's need to break down hemoglobin within the red blood cell. The most widely accepted is the need for the amino acids from the globular portion of the protein. The fact that the concentration of free amino acids in infected cells is much higher than in uninfected cells and that radio-labeled amino acids in infected cells later appeared in the parasite it self support this. Another reason for the breaking down of hemoglobin is also to make room within the cell to allow the parasite to grow [2].

The Pathway from Hemoglobin to Hemozoin

The process to break down the hemoglobin is a very complex one. The details of the actual pathway are debated. The process involves: transport of the hemoglobin from the cell cytosol to the food vacuole, the breakdown of the hemoglobin tetramer, the removal of the heme moiety, the detoxification by forming hemozoin, and the final breakdown of the amino acids chains [2]. The formation of hemozoin from the free hemes is an important step as the free-heme is toxic to the parasite.

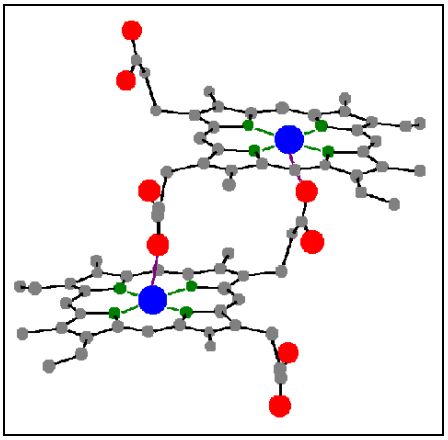

Figure 6: Ball and stick representation of beta-hematin [14]

Hemozoin

The hemes removed from the globular portion of the protein are turned into hemozoin by the parasite. The structure of hemozoin is formed by pure heme without the rest of the protein. It has been shown that hemozoin is structurally identical to synthetic β-hematin. Wood and McNaughton confirmed this by taking the Raman spectra of both and they match within a wave number.

CHAPTER THREE: EXPERIMENTAL SETUP

General

The goal of this research is to develop a technique using capillaries to study red blood cells *in vivo*, specifically those infected with the malaria parasite. This is accomplished by, first placing both the healthy (uninfected) and infected cells on traditional slides under a confocal Raman microscope and comparing the spectra to previously obtained published spectra. Samples are then placed in capillaries and examined to look for differences and similarities. The two techniques are then compared for future possibilities.

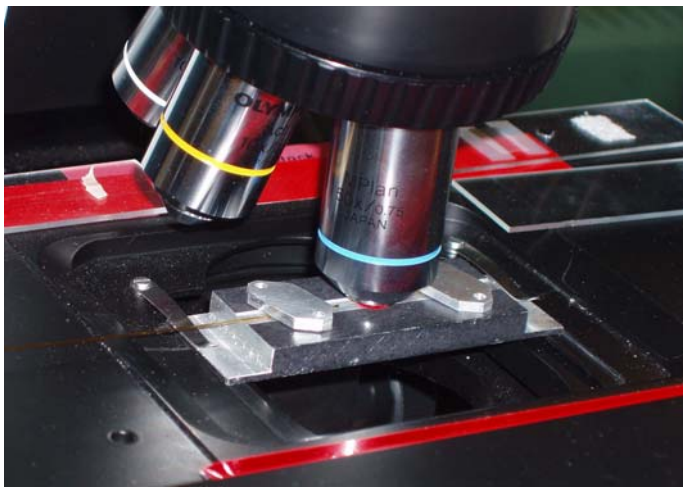

Figure 7: Capillary on stage

Experimental Apparatus

Raman spectra were taken using a helium:neon (He:Ne) laser (4 mW), at 632.8nm put through a confocal microscope (Olympus BX41) equipped with a 100x objective (NA = 0.9, Leica HCX PL). The scattered light is collected back through the same optical system and then sent through a holographic notch filter (to remove the Rayleigh line) and then to a 100 μm

pinhole and 600 grating. The spectral analysis is done using a Jobin Yvon spectrometer (HR800UV) with a CCD camera cooled to -84ºC.

Figure 8: Jobin Yvon LabRAM HR Setup

Samples

Preparation

The samples were prepared by the group of Dr. D. Chakrabarti in the University of Central Florida's Department of Molecular Biology & Microbiology. *Plasmodium falciparum* parasites (3D7 strain) were maintained at 4% hematocrit in RPMI1640 supplemented with 0.5% Albumax, 0.2% dextrose, 0.1 M NaHCo3 and 25mg/ml gentamycin prior to Raman spectroscopy. Infected cultures were either smeared onto glass slides, or washed three times in 1xPBS, pH 7.2 and enclosed in micro-capillaries for Raman spectroscopy. Uninfected samples were prepared from the same blood source for comparison and prepared using the same method.

The samples were transported directly to the Raman lab. All data was collected within approximately 2 hours after samples preparation. Because of this the Raman set up was calibrated beforehand using a silicon sample to check signal strength and Naphthalene crystals to

calibrate the spectrometer. The samples on slides were observed through the microscope directly. The samples enclosed on micro-capillaries were prepared by placing the prepared 50 x 50 μm square capillary into the culture and allowing capillary action to draw the cells up. This usually resulted in 10-15 individual cells in the viewing window. This was a perfect amount to allow for enough cells for viewing but not so many that they interfered with each other.

Slide Samples

The slide samples were prepared in order to provide a standard with which to compare spectra from the literature. The samples were prepared in a similar manner to those that would be prepared in any laboratory for the detection of Malaria. The exception is that there were slides prepared and stained for the observation of the parasite to first confirm their presence and then slides made with out staining for use in the Raman system.

Capillaries

The novel use of capillaries to study the cell *in vivo* is one of the key elements of this study. The capillaries are 50 x 50 μm fused silica square tubes produce by Polymicro Inc (Part #2001513). Square tubes were chosen for better viewing quality than round tubes.

The capillary samples were prepared by first cutting them off of the roll with a sharp knife. The middle portion was heated to removed the protective coating and allow for viewing the sample inside. Care must be taken once the coating is removed as the capillaries are very fragile at that point. The end of the capillary was placed in the infected solution for approximately 3 minutes. This was enough time to allow the natural capillary action to draw up enough cells for viewing.

Collection

The samples were placed under the microscope and positioned visually using the CCD camera and 3-D translational stage. A photograph of the cell was taken and then the light and camera were turned off and the camera's mirror removed. The 633nm beam was then turned on. The beam spot at the sample, due to the confocal setup, is approximately 1 x 2 μm. The exposure time to the laser was kept to a minimum to prevent photo-induced effect (such as photolysis of bound ligands, etc.) Data collection times were set at 20 sec per accumulation to prevent saturation of the CCD. Each data set was the total of 5 accumulations.

CHAPTER FOUR: RESULTS

The results are presented here. The uninfected cells, both traditional slides and in capillaries, are shown first. These are followed by the infected samples. Several spectra are presented for each sample, each of which was taken from a different random cell for comparison.

Uninfected Red Blood Cells

Uninfected Slides

The 600-1200 cm^{-1} region is known as the low-wavenumber region. The intense peak at 754 cm^{-1} is attributed to a pyrrole breathing mode and is seen in both oxygenated and deoxygenated cells and also is present in hemozoin. The peak at 787 cm^{-1} is present, although weak as usual, and assigned to another pyrrole breathing mode. The dual peaks near 978 cm^{-1} and 996 cm^{-1} are assigned to an asymmetric pyrrole deformation mode and a C-C stretching vibration. The peak at 1172 cm^{-1} is assigned to a half-ring stretching mode and is also present.

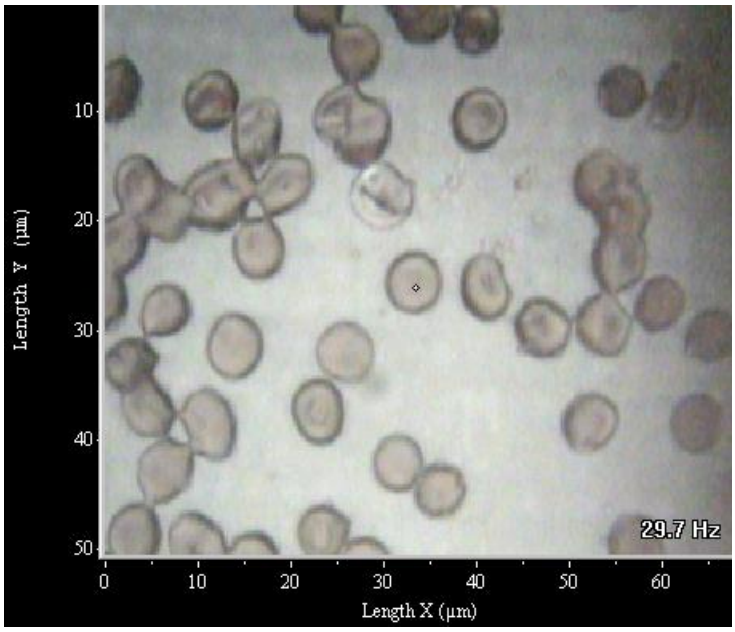

Figure 9: Red blood cells (slide)

In the C-H deformation region from 1200-1300 cm^{-1} the major feature is the peak at 1225 cm^{-1}. This peak is due to C-H stretching. There is a band near 1245 cm^{-1} that blends with the 1225 peak. It is also attributed to a C-H stretch mode.

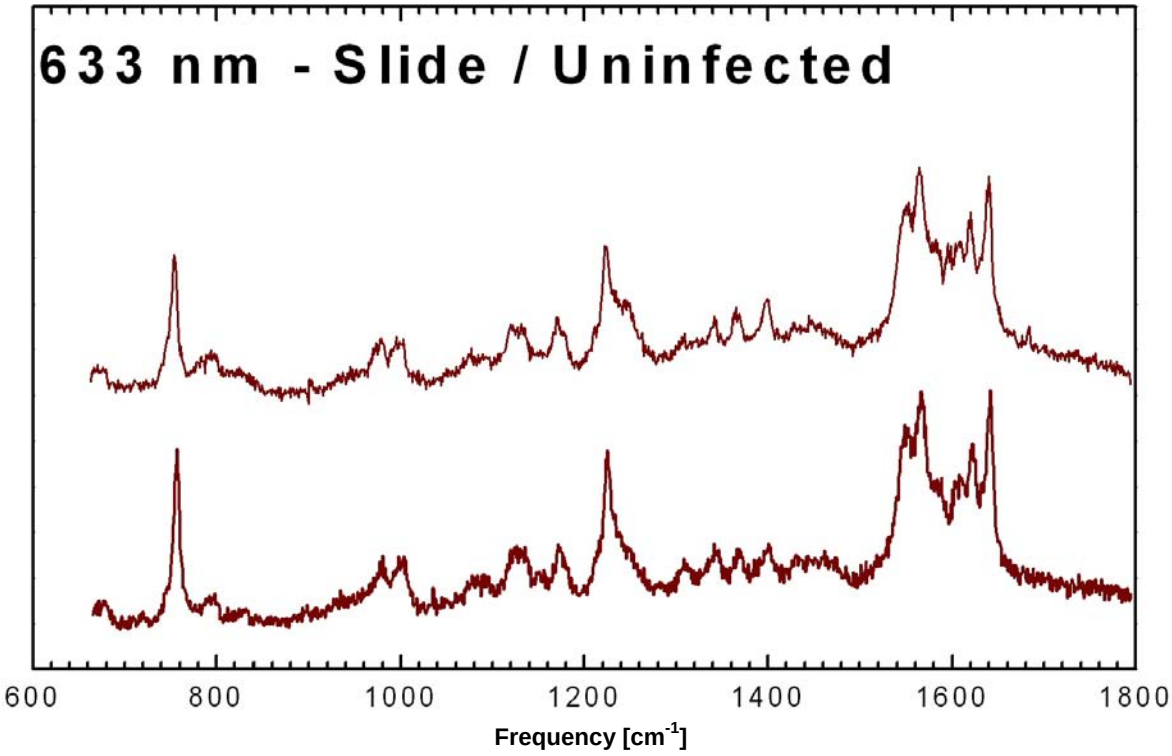

Figure 10: Raman spectra of single uninfected red blood cell (slide)

The 1300-1400 cm^{-1} band includes three modes of pyrrole ring stretching. The three peaks represent different phases of the vibrations. The 1341 cm^{-1}, 1366 cm^{-1}, and 1399 cm^{-1} bands are all of nearly equal intensity. These bands are also independent of oxidation state.

The 1500-1650 cm^{-1} band contains most of the core size or spin state markers. The significant peaks in this band are at 1548 cm^{-1}, 1565 cm^{-1}, 1608 cm^{-1}, 1621 cm^{-1}, and 1640 cm^{-1}. These peaks are representative of those seen in oxygenated cells as these bands are dependent on oxidation state. All of the peaks in this region are assigned to C-C stretching in the pyrrole ring which is why they are so dependent on whether the heme has bound oxygen.

Uninfected Capillaries

The capillary samples exhibited the same low wavenumber characteristics as the slides. The intense peak at 754 cm^{-1} is still prominent, although slightly lower in intensity as is the peak at 787 cm^{-1}. The dual peaks near 978 cm^{-1} and 996 cm^{-1} are clear. The peak at 1172 cm^{-1} is also present.

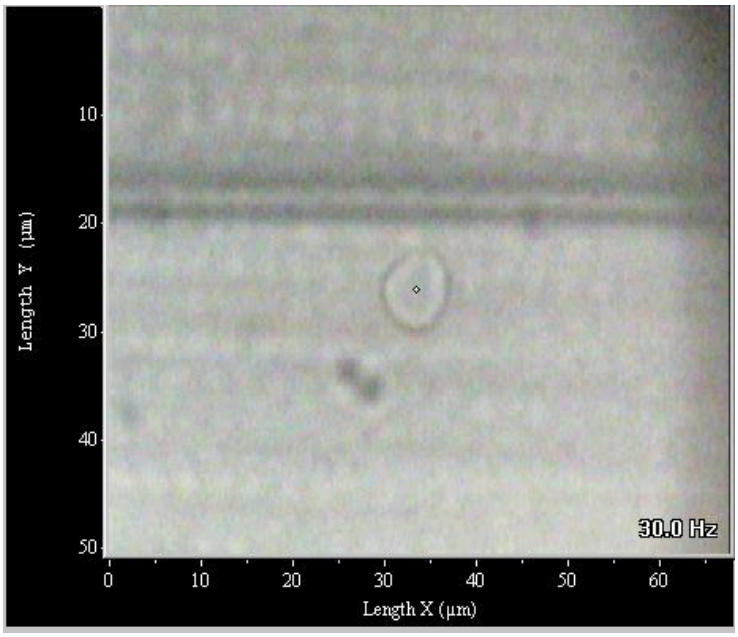

Figure 11: Red blood cells (capillary)

In the region from 1200-1300 cm^{-1}, the peak at 1225 $cm^{-1}$is still there. There is a peak at 1210 cm^{-1} clearly seen in the capillary spectra. This peak is also partially seen in the infected capillary samples. The band at 1245 cm^{-1} that blends with the 1225 peak is still visible.

The three modes of pyrrole ring stretching from 1300-1400 cm^{-1} are present although slightly weaker. The relative intensities are more equal than in the slide sample.

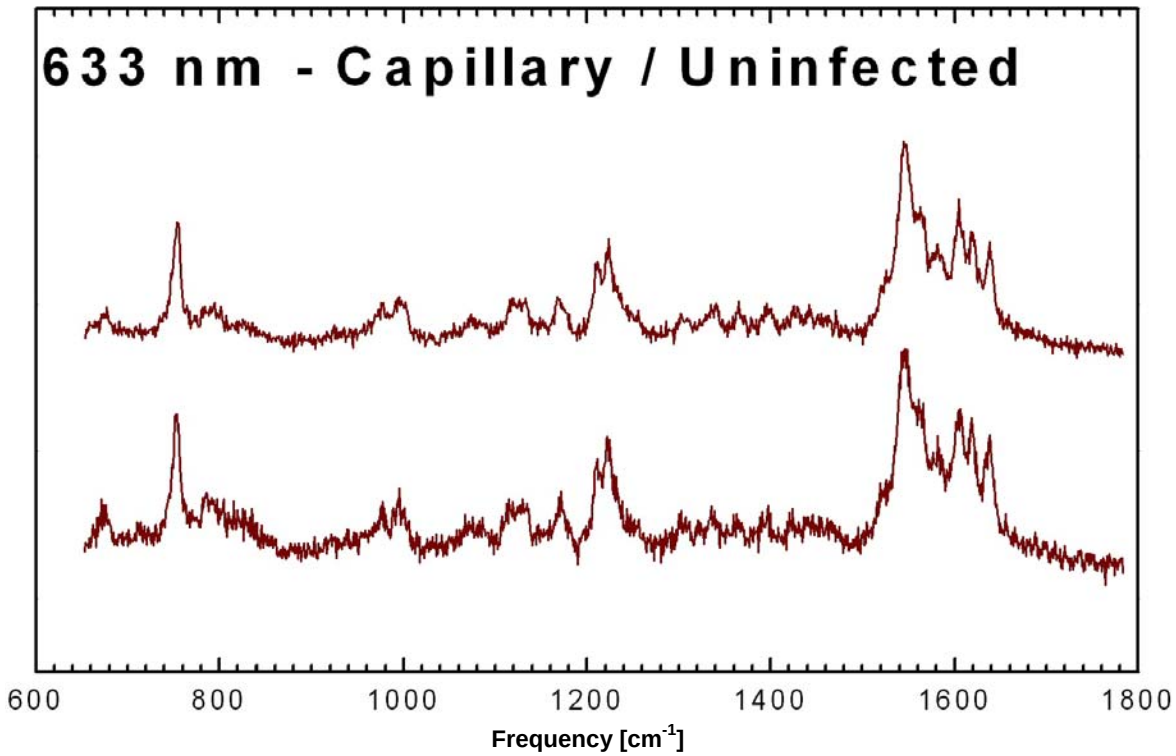

Figure 12: Raman spectra of single uninfected red blood cell (capillary)

The range from 1500 cm^{-1} to 1650 cm^{-1} contains the most significant differences. The significant peaks seen in the capillary sample are at 1546 cm^{-1}, 1563 cm^{-1}, 1604 cm^{-1}, 1618 cm^{-1}, and 1638 cm^{-1}. The overall structure of this entire band is visibly different. The reasons are not immediately clear.

Infected Red Blood Cells

Now that the system is calibrated and can reproduce published results, the next step is to test red blood cells infected with *Plasmodium falciparum* both on slides and then using the micro-capillaries. Infected red blood cells were prepared on a slide for comparison with uninfected slides and then examined in the capillaries to test the technique. That data is presented here.

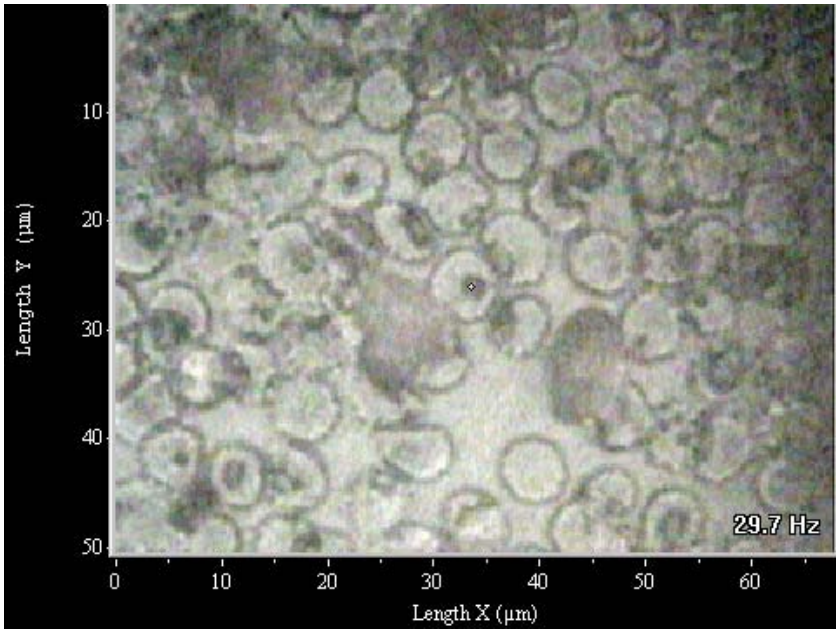

Figure 13: Plasmodium falciparum infected red blood cells (slide)

Infected Slides

The low-wavenumber region appears very much unchanged. The peak at 754 cm^{-1} is still present although it appears much more broadened. The peak at 787-790 cm^{-1} is present, although it appears weaker than in uninfected cells although the presence of more noise in this signal is most likely the reason. The peak at 978 cm^{-1} is shifted down nearly 10 cm^{-1} and the 1001 cm^{-1} peak is unchanged. The band at 1173 cm^{-1} is unchanged.

As stated before, the major feature in the C-H deformation region (1200-1300 cm^{-1}) is the peak at 1225 cm^{-1}. This peak is due to C-H stretching and appears greatly changed. The number of photon counts is proportionately the same at 1225 cm^{-1}. There is, however, a broad band signal that appears next to it. This could be the 1225 cm^{-1} line shifting to the right or a drastic strengthening of the band centered near1248 cm^{-1}. This peak is also attributed to a C-H stretch mode.

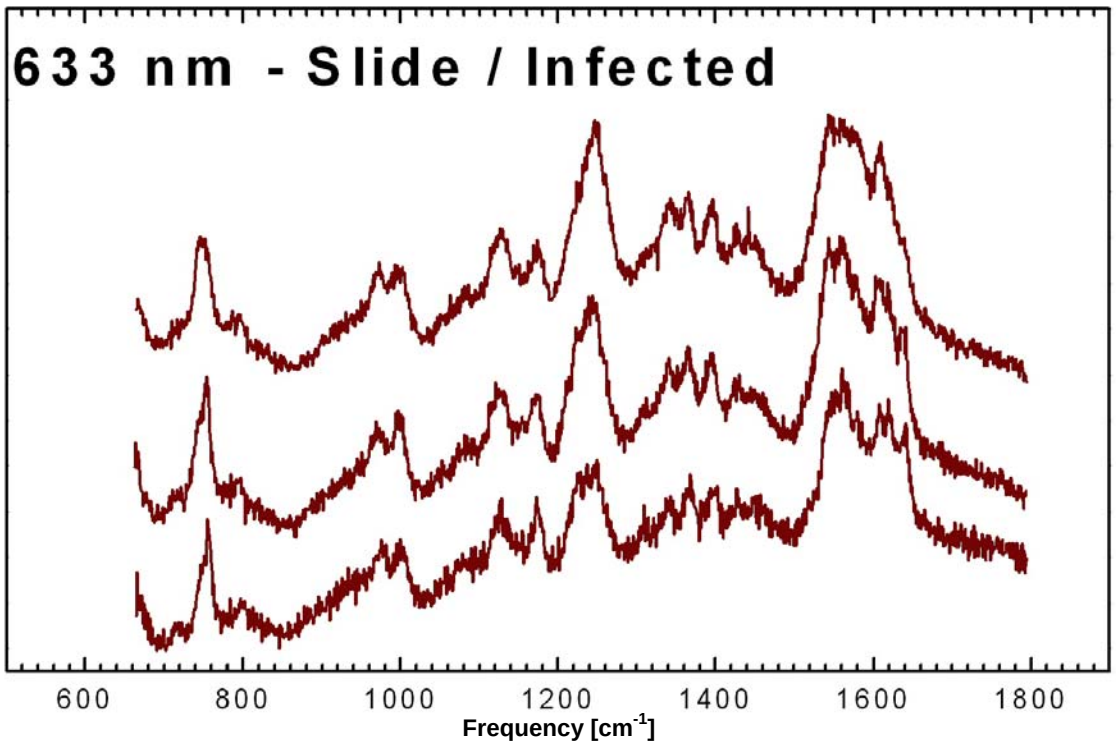

Figure 14: Raman spectra of a Plasmodium falciparum infected cells (slide)

The three modes of pyrrole ring stretching (1300-1400 cm^{-1}) occurring at 1341 cm^{-1}, 1366 cm^{-1}, and 1399 cm^{-1} bands are all appeared in the infected cells. They are still each of nearly equal intensity to each other but appear relatively stronger compared to the rest of the spectrum signal.

In the 1500-1650 cm^{-1} band there appears the greatest changes. The significant peaks for this sample appear at 1545 cm^{-1}, 1563 cm^{-1}, 1607 cm^{-1}, 1621 cm^{-1}, and 1640 cm^{-1}. The peaks in this band are also broader than in the uninfected samples.

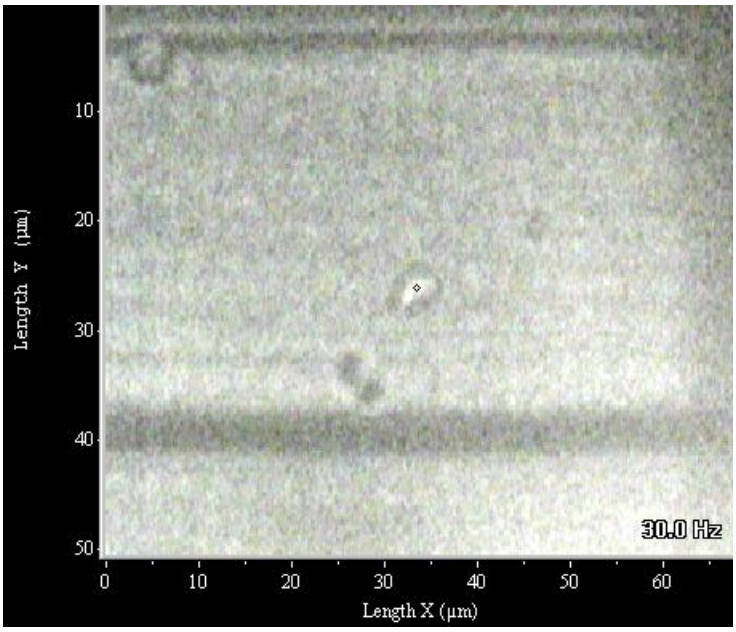

Figure 15: Infected cell in capillary

Infected Capillaries

First a spectrum of an empty capillary was taken to provide a background signal and to ensure there were no unpredicted Raman signals. This background signal was taken while focusing the beam spot above the capillary's upper surface, inside the upper surface, and inside the empty capillary. As expected, there were no detectable signals present thus indicating the capillary itself should not interfere with the spectrum of the samples.

With the cell in the capillary the low-wavenumber region appears very similar to the infected slide sample. The peak at 754 cm^{-1} is present and is still broadened when compared to the uninfected sample. There is an interesting side peak at 744 cm^{-1} that does not appear in either of the other samples or in the literature and could explain the broadening seen in the infected slide sample. The peak at 787-790 cm^{-1} is again obscured by noise as with the infected slide sample. The bands near 1000 cm^{-1} are also very similar to the infected slide.

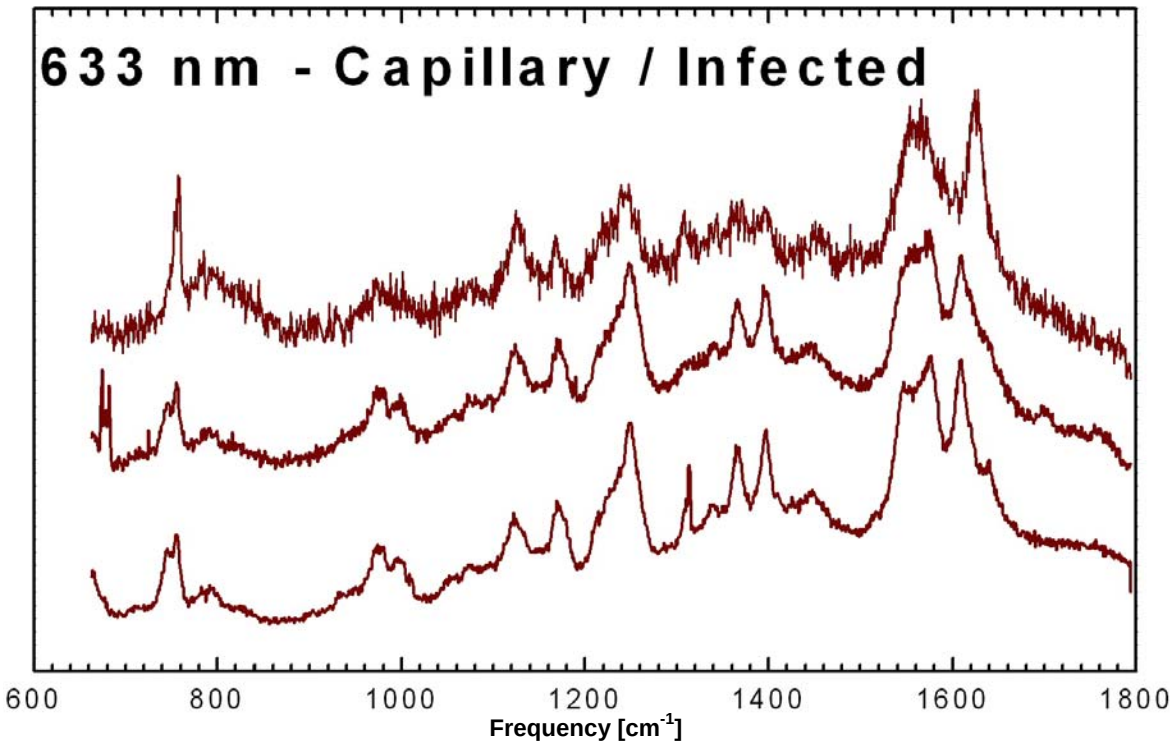

Figure 16: Raman spectra of a Plasmodium falciparum infected cell (capillary)

In all, the 1000- 1300 cm^{-1} peaks are unchanged from the infected slide sample with the exception of the major peak at 1225 cm^{-1}. This peak is very much reduced.

Within the 1300-1400 cm^{-1} band the first of the three pyrrole ring stretching modes is almost not existent.

The 1500-1650 cm^{-1} band shows some of the most drastic differences. The significant peaks in this band are at 1545 cm^{-1} (reduced), 1563 cm^{-1} (unchanged from before), 1607 cm^{-1} (unchanged), 1621 cm^{-1} (reduced), and 1640 cm^{-1} (reduced). There is also a notable gap in the spectrum 1585-1602 cm^{-1}.

CHAPTER FIVE: DISCUSSION

Verifying the Experimental Setup

System Calibration

This study began by running calibration spectra using healthy red blood cells on standard glass slides to ensure that reproducible results were obtainable. The spectrum seen from red blood cells is dominated by that of hemoglobin and is well studied and documented. The spectra obtained from healthy red blood cell fixed on glass slides were in very good agreement with published data (see table 1.)

Table 1: Oxygenation State of Healthy Cells

Assignments (Abe [16])	Healthy Slide	Oxy (Wood [8])	Deoxy (Wood [8])
ν_{10}	1641	1638	Absent
$\nu_{(C=C)}$	1622	1618	Absent
ν_{19}	1607	1604	1608
ν_{37}	1587	1581	1585
ν_{2}	1566	1565	Absent
ν_{11}	1547	1546	1544
ν_{28}	1430	1428	1426
ν_{20}	1400	1398	1398
ν_{4}	1369	1367	1365
ν_{41}	1342	1342	1340
ν_{21}	1308	1306	1306
ν_{13}	1250	1249	Absent
ν_{42}	1225	1226	1223
ν_{30}	1172	1172	1171
ν_{22}	1127	1129	1123
ν_{23}	1090	1090	1084
ν_{47}	997	996	996
ν_{46}	978	978	972
ν_{6}	792	787	790
ν_{15}	756	753	752
ν_{7}	671	668	672

The assignments listed in the table are labeled using the same system of described by Abe *et al* [16] to facilitate comparison with the literature. All of the important features of the hemoglobin vibrational spectrum at 633 nm are seen.

Next, Raman spectra of empty capillaries were taken to ensure that no interference from the capillary would be seen. At the 633 nm wavelength used in this experiment, however, no measurable Raman signal was detected from the fused silica. This is also most likely due to the confocal setup that ensures that the only measured spectrum is in the sample volume. Measurements were taken while focusing from above the outer surface of the capillary through to the lower side. This indicates that the capillaries should not interfere with the data. There were, however, some interesting effects seen when the samples were analyzed in the capillaries. These will be discussed shortly.

Determining the Oxygenation State

The next step in the process was to determine the oxidation state of the hemoglobin present in the cells. Because no special steps were taken to ensure that the cells were deoxygenated and blood samples are usually drawn from a subject arterially it was assumed prior to beginning that bound oxygen would be present. The high binding affinity of oxygen to the heme means that the oxygen, once bound, will not easily disassociate without some catalyst. From the healthy spectra taken on glass slides the peaks indicate that the cells sampled are mostly oxygenated (see table 1.) This is important as it has been shown that the oxidation state of the heme has a significant impact on the resulting spectra [8].

Malaria Detection

Presence of Hemozoin

One of the prime targets for determining the presence of the Malaria parasite is the presence of the waste product hemozoin. The crystallized hemozoin is collected by the parasite and excreted into a vacuole to protect itself from the toxic nature of the waste product. The structure of hemozoin is identical to the artificially manufactured β-hematin and therefore has an identical Raman structure [17]. Finding the characteristic peaks of hemozoin can identify the presence of Malaria. The data taken from the infected cells on a slide are shown in table 2 and are compared (on either side) with the nearest peaks from both hemoglobin and hemozoin spectra (nearby peaks are defined as "within +/- 3 cm^{-1}.")

The spectra from the infected cells match those of normal hemoglobin within 3 wavenumbers throughout most of the range presented here. This indicates that the spectrum is nearly made up of healthy hemoglobin. In the low wavenumber region there are two peaks (972 cm^{-1} and 796 cm^{-1}) that are seen in the slide sample that do not appear in normal hemoglobin but do match those of hemozoin. Theses peaks correspond to the pyrrole deformation mode and one of the pyrrole breathing modes respectively.

The reason for the absence of a clear hemozoin spectrum is puzzling. The brown tinted hemozoin crystals produced by the trophozoite stage parasites were visible under light microscopy. One possible explanation could be some small misalignment between camera (used for targeting) and the laser causing the spectra to be recorded from some neighboring spot within the cell. This was checked by targeting above, below, and to either side of the vacuole. Any alignment error should have been detected, none was.

Table 2: Comparison of Hemoglobin, Hemozoin, and infected slides cells

Hemoglobin (Wood [8])	Infected Slide Cells	Hemozoin (Wood [17])
1638	1638	-
1618	1619	-
1604	1604	-
1581	1578	1581
1565	1563	-
1546	1545	-
1428	1427	1430
1398	1396	1398
1367	1366	-
1342	1343	-
-	1310	1308
1249	1249	-
1226	1225	-
1172	1174	-
1129	1131	-
1090	1087	-
996	998	-
-	972	971
-	796	797
-	757	754

Hemoglobin Degradation

Another feature of the spectra is the degradation of the hemoglobin. Figure 17 shows the comparison of a healthy sample and an infected sample. The most obvious features are the broadening of all the major bands and the changes in the 1618 and 1638 cm^{-1} peaks. Why these appear is just as curious. The two are associated with heme modes and may result from the heme's release from the protein before the formation of a complete hemozoin crystal.

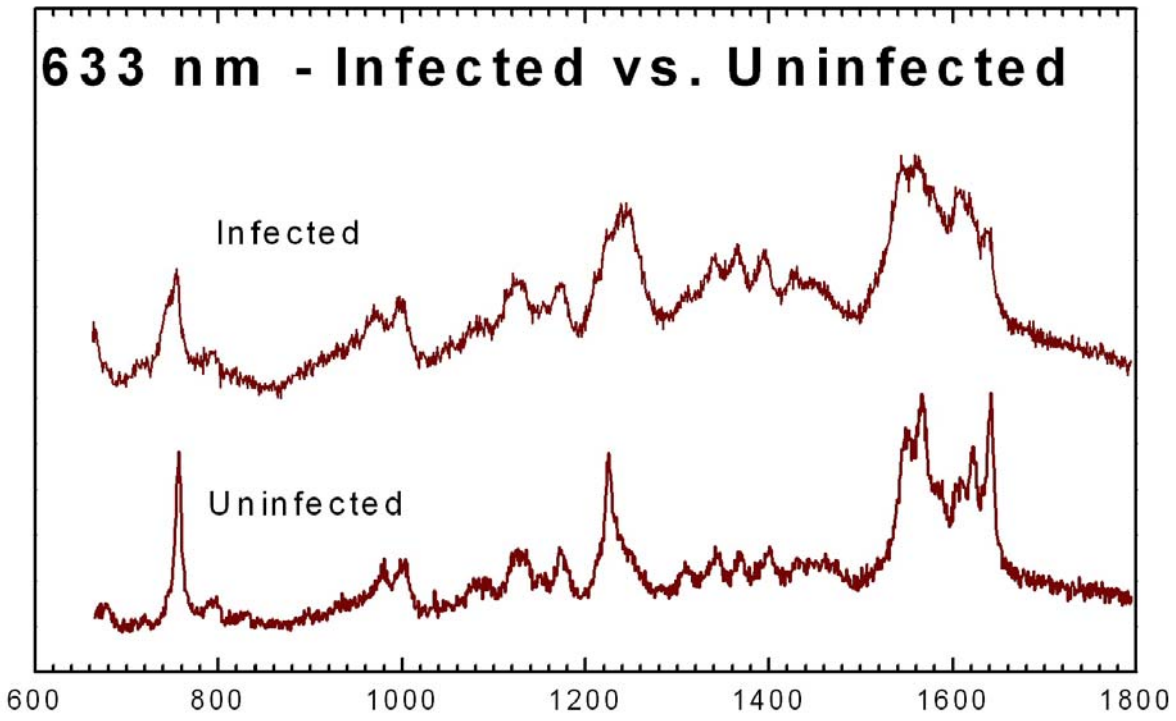

Figure 17: Comparison of infected and uninfected cells (slides)

As the hemoglobin is broken down by the parasite, the protein chain fragments are transported away for further digestion. The remaining toxic heme is then oxidized to a ferric state. The release of the heme from the protein is the first step in the formation of hemozoin. The changes in the spectra could be the result of this degradation and the changes in the vibrational modes of the now free heme. As the heme rings are no longer bound within the pocket of the protein the constraints on the various bonds will be much more random and could account for the broadening of the bands. Further evidence of this is that when the cell was exposed to the laser beam over long periods of time (>60 seconds) the spectra tended to change with time and Although this in not conclusive evidence of the presence on the malaria parasite it is a signal that changes are taking place in the heme structure.

To check this, a cell that appeared to be uninfected (i.e. in an infected sample, however, with no visible presence of hemozoin) was sampled and then left under constant exposure to the laser for one minute and then sampled again. This process was repeated four times. The data is shown in figure 18.

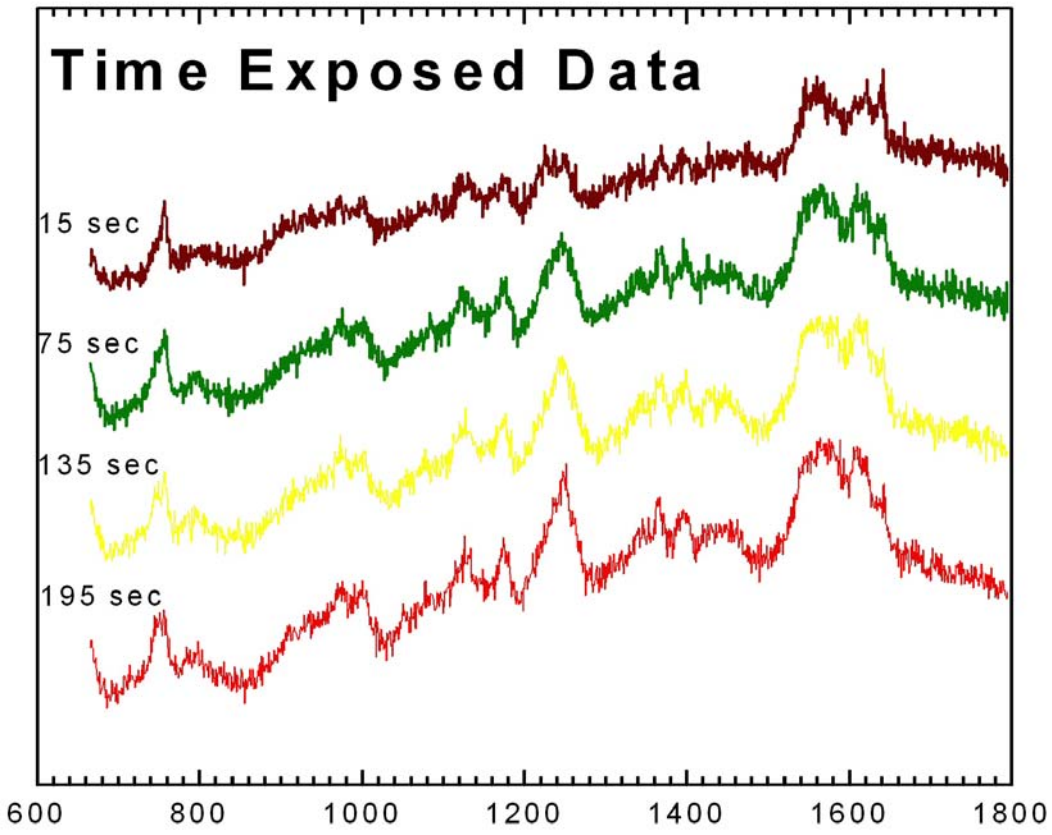

Figure 18: Time exposed cells

The spectra change over time. It starts with all of the characteristics of a healthy sample cell with normal hemoglobin. Over time the spectra shifts more towards the spectra from an infected cell with the broadening of the key peaks and the reduction in intensity in the 1600-1700 cm^{-1} range. This supports the idea that the changes in the spectra in the infected samples are indicative of degrading hemoglobin.

The Use of the Capillaries

Success of Capillary Technique

The use of capillaries to study the red blood cells can be considered somewhat successful. The cells are allowed to remain in a state much more closely resembling their native environments. They are easily introduced to the capillaries and they were easy to find and observe. The fact that they were not put on a slide open to the air and fixed kept them alive, if only for a short time. They moved only slightly once inside the capillary but usually not outside of the viewing area. The spectra obtained from the slides prepared in the traditional manner and the spectra obtained from the capillaries were nearly identical when looking at the infected cells (figure 19.) However, when comparing the uninfected cells there was a change that is not easily explainable.

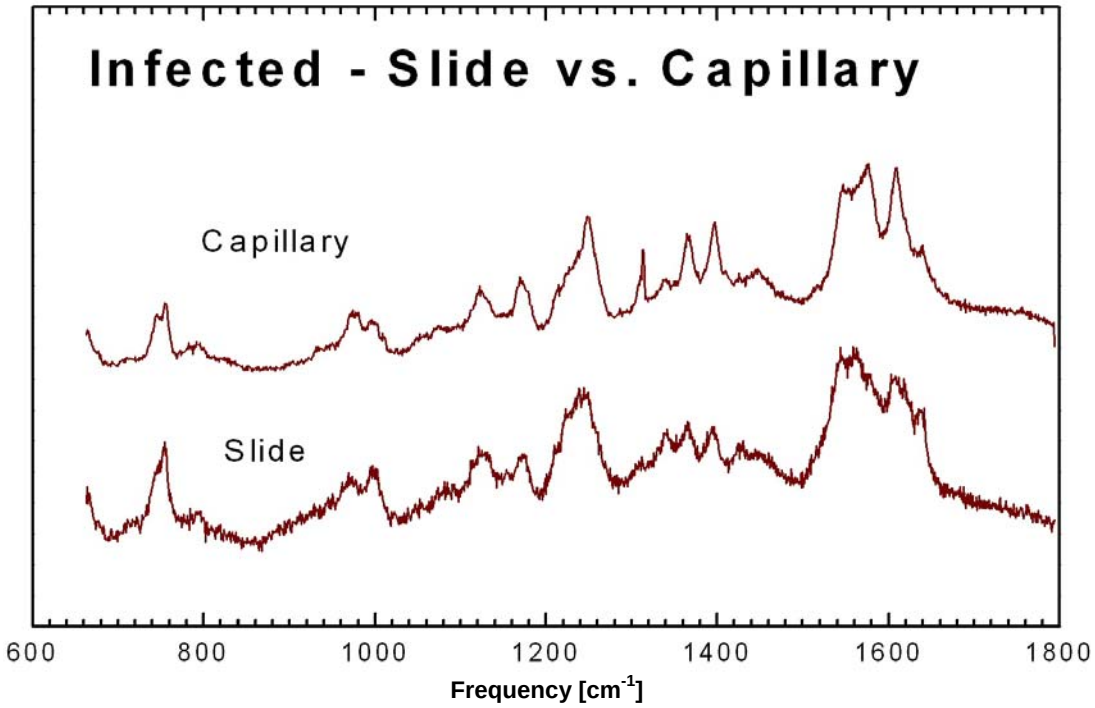

Figure 19: Comparison of capillary spectrum with slide (both infected cells)

The uninfected samples show a change in the 1600-1650 cm^{-1} region. The change is notable not only because it may indicate that the capillary may be blocking some of the scattered light but also because the change is similar to that in degraded hemoglobin. The spectra in figure 20 are taken from healthy cells so there should be no degradation due to the parasite. This may indicate that the cells in the capillary are breaking up and the hemoglobin is beginning to degrade on its own.

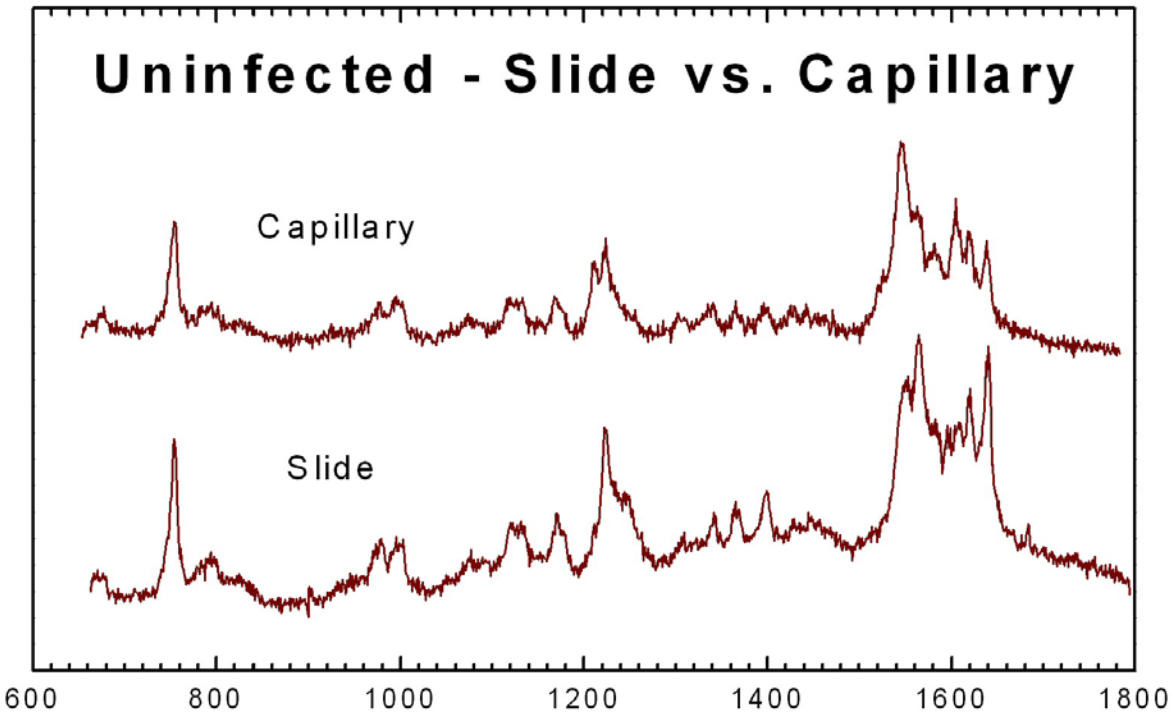

Figure 20: Comparison of healthy slide and capillary

Future Uses for the Capillaries

The potential applications of using this technique are wide. The capillaries could be closed of and stored in a manner to keep the cells and their parasites alive. Inside the capillary the cells are spread out and this allows for the analysis of individual cells with out interference from neighbors. Blood with washed and separated cells (like the ones used here) or blood in bulk could be flowed through under pressure and allow for even more realistic *in vivo* studies.

In this study the end of the capillaries were left open and then they were observed within 2 hours of preparation to ensure the cells and parasites were still alive. By closing off the ends of the capillary and storing them appropriately the entire system inside could be kept alive for extended periods allowing for repeated Raman studies of the same cell. The changes over time and throughout the life cycle of the parasite could be studied. Observations could be made during the cells rupture to elucidate structural changes during this still mysterious phase of the life cycle.

When the cells are drawn into the capillary they are much more spread out than when observed on slides. This allows for individual cells to be observed without interference from other nearby cells. On a slide cells are fixed in position and relocating a specific cell is relatively easy. This is done by either referencing the neighboring cells or tracking the position of the camera with the microscope's translational stage. If the cells are allowed to move this becomes nearly impossible to do with out some form of chemical marker, which of course must disturb the system. The low density of the capillary cells allows for easy tracking of specific cells. This is particularly useful when trying to make repeated measurements of the same target.

Although up to five times larger than actual human blood capillaries, the fused silica capillaries used in the study could be used to examine bulk blood and determine the capability of the system to analyze the cell as they flow by combining the current technique with statistical model and averaging. The flow would pass different cells through the sampling volume and the statistics of this flow would have to be accounted for. This would be the next step in finding a true *in vivo* diagnostic tool for the detection of infected cells.

CHAPTER SIX: CONCLUSION

Micro-Raman measurements using 632.8 nm excitation radiation were taken on several samples of red blood cells under different conditions for comparison. The spectra showed the high signal to noise ratio needed for structural analysis. The confocal system provided the ability to precisely target individual points within the cell in all three axes. The spectra taken of uninfected cells on a glass slide using traditional preparation methods were taken to calibrate the system and verify that previously published data could be reproduced. Spectra were taken of cells infected with the Malaria parasite *Plasmodium falciparum* in an attempt to locate differences in the spectra that would allow for the study of structural changes in the hemoglobin protein. The hemoglobin spectra showed clear differences between the healthy and infected samples. The changes were similar to that seen during the degradation of the hemoglobin and may be caused by the parasites catabolism of the protein. Further, the cells were placed in fused silica capillaries to simulate a more native-like environment than prepared and fixed on a glass slide. The capillary spectra were very similar to the slide's but showed a , as of yet, unexplained reduction in intensity in the 1600-1650 cm^{-1} range.

Research will continue by examining the structural changes of the hemozoin and looking for relationships between these changes and the growth cycle of the parasite. The experimental set up will be improved allowing for the ability to conduct raster scans of entire cells allowing for better comparison of the infected site and non-infected sites within the same cell. The capillary technique will continue to be refined. The use of capillaries can be expanded by exploring the capability to keep the cells alive allow for a continued study of the same cells over long periods of time. This will allow the growth of parasite to be monitored and Raman data collected

throughout its life cycle, a technique not viable for cell fixed on slides. This may lead to methods for detecting the parasite before it is even visible to the laboratory technician under stain leading to almost instantaneous detection of infections.

Understanding the structural changes in the degradation of hemoglobin may open new targets for anti-malarial drug treatments. By observing the cells in a native-like environment may lead to the ability to carry out this analysis of cells while still in the human body leading to easier, faster detection of the parasite's presence. This method could be combined with current research in *in vivo* techniques currently be developed using fiber-optic Raman system to produce a lightweight field unit for parasite detection.

LIST OF REFERENCES

1. U.S. Department of Health and Human Services, "Understanding Malaria", NIH Publication No. 07-7139, February 2007.

2. W. Sherman, ed. "Molecular Approaches to Malaria", ASM Press, Washington D.C., 2005.

3. Center for Disease Control, http://www.dpd.cdc.gov/dpdx/HTML/ImageLibrary/Malaria_il.htm, (Cited May 20, 2007).

4. World Health Organization, "Malaria Light Microscopy, Creating a Culture of Quality", SEARO/WPRO Workshop, Kuala Lumpur, Malaysia, 18–21 April 2005

5. Kyowa Optical, Retrieved from http://www.kyowaopt.co.jp/English/malaria/malaria.htm, (Cited May 20, 2007).

6. New Perspectives: Malaria Diagnosis. A joint WHO/USAID informal consultation 25-27 October 1999.

7. B. F. Brehm-Stecher, E. A. Johnson, "Single-Cell Microbiology: Tools, Technologies, and Applications", Microbiol. Mol. Biol. Rev. Sept. 2004, p. 538–559.

8. B. R. Wood, D. McNaughton, "Raman excitation wavelength investigation of single red blood cell in vivo", J. Raman Spectrosc. 2002; 33: 517–523

9. B. R. Wood, D. McNaughton, "Raman Spectroscopy in Malaria Research", Expert Rev. Proteomics 3(5) 2006.

10. McCreery, "Raman Spectroscopy for Chemical Analysis", Wiley-Interscience, New York, 2000.

11. J.J. Laserna, ed. "Modern Techniques in Raman Spectroscopy", John Wiley & Sons, New York, 1996.

12. Y.Guo, PhD Thesis, University of Central Florida, 2006.

13. D. R. Vij, ed. "Handbook of Applied Solid State Spectroscopy", Springer, New York, 2006.

14. M. Wiser, "Ball and Stick Representation of β-hematin", Retrieved from http://www.tulane.edu/~wiser/malaria/heme.html (Cited May 20, 2007).

15. B. R. Wood, B Tait, D. McNaughton, “Micro-Raman characterisation of the R to T state transition of haemoglobin within a single living erythrocyte”, Biochimica et Biophysica Acta 1539 (2001) 58-70.

16. M. Abe, T. Kitagawa, K. Kyogoku, “Resonance Raman spectra of octaethylporphyrinato-Ni(II) and meso-deuterated and ^{15}N substituted derivatives.” J. of Chemical Physics 69 (1978) 4526-4534

17. B. Wood, et al. “Raman imaging of the Raman imaging of hemozoin within the food vacuole of Plasmodium falciparum trophozoites”, FEBS Letters Vol 554 Issue 3 (2003) 247–252